Int. J. Heat Mass Transfer. Vol. 11, pp. 241–253. Pergamon Press 1968. Printed in Great Britain

AN ANALYSIS OF LAMINAR FREE CONVECTION FLOW AND HEAT TRANSFER ABOUT AN INCLINED ISOTHERMAL PLATE

WITOLD T. KIERKUS

Institute of Heat Engineering, Warszawa, Nowowiejska 25, Poland

(*Received* 29 *March* 1967)

Abstract—The paper presents a perturbation analysis for two-dimensional laminar free convection about an inclined isothermal plate, using the classical boundary-layer solution as the zeroth-order approximation. First-order perturbation solution has been found for the velocity and temperature fields. The distributions of both components of the velocity field and temperature field, calculated in detail for Prandtl number 0·7 and inclination angles $\varphi = 0, \pm 15, \pm 30, \pm 45$ are compared with experimental data. Good agreement is found between the theoretical solution and experimental results.

NOMENCLATURE

a, thermal diffusivity of fluid [m^2/s];

$F(\eta)$, dimensionless boundary-layer stream function;

$f(\eta)$, $f_m(\eta)$, dimensionless functions introduced in equation (26);

g, acceleration due to gravity [m/s^2];

$H(\eta)$, dimensionless boundary-layer temperature function;

$h(\eta)$, $h_m(\eta)$, dimensionless functions introduced in equation (27);

L, length of the plate [m];

m, dimensionless exponent introduced in equation (25);

N_{Gr}, Grashof number, $N_{Gr} = \dfrac{g\beta(T_w - T_\infty) L^3 \cos\varphi}{\nu^2}$;

$\bar{N}_{Gr}$, local Grashof number, $\bar{N}_{Gr} = \dfrac{g\beta(T_w - T_\infty)\bar{x}^3}{\nu^2}$;

N_{Nu}, local Nusselt number, $\bar{N}u = \dfrac{\alpha\bar{x}}{\lambda}$;

N_{Pr}, Prandtl number, ν/a;

p^+, $P(X, Y)$, dimensionless pressure difference defined by equation (9);

$p(\eta)$, $p_m(\eta)$, dimensionless functions introduced in equation (28);

$\bar{p}$, static pressure [N/m^2];

$\bar{T}$, temperature [degK];

$\bar{T}_r$, reference temperature for evaluating physical properties of fluid [degK];

U, dimensionless potential flow velocity component in $\bar{x}$ direction;

$\bar{u}$, velocity component in $\bar{x}$ direction [m/s];

V, dimensionless potential flow velocity component in $\bar{y}$ direction;

$\bar{v}$, velocity component in $\bar{y}$ direction [m/s];

x^+, X, dimensionless coordinate along the plate surface;
$\bar{x}$, coordinate along the plate surface, measured from the leading edge [m];
y^+, Y, dimensionless coordinate normal to the plate surface;
$\bar{y}$, coordinate normal to the plate surface, measured from the plate [m].

Greek symbols

α, local heat-transfer coefficient [W/m^2 degK];
β, coefficient of thermal expansion of fluid, $-\left(\frac{1}{\rho}\frac{\partial\rho}{\partial T}\right)_p$ [degK^{-1}];
η, dimensionless independent variable defined by equation (22);
$\theta(X, Y)$, dimensionless temperature function defined by equation (9);
λ, thermal conductivity of fluid [W/m degK];
ν, kinematic viscosity of fluid [m^2/s];
ρ, density of fluid [kg/m^3];
φ, plate surface inclination angle;
$\psi(X, Y)$, dimensionless stream function defined by equation (9);
ψ^+, dimensionless stream function.

Superscripts

(1), (2), (3), perturbations orders;
$'$, derivatives with respect to η.

Subscripts

∞, ambient conditions;
w, wall conditions.

INTRODUCTION

RECENTLY, theoretical studies of laminar free convection have received much attention, especially in cases of different geometry of the surface. These analyses, except the one by Yang and Jerger [1] done by perturbation solution, are based on laminar boundary-layer equations, which are only adequate for large Grashof numbers, more precisely, they represent asymptotic solutions to the complete Navier–Stokes, continuity and energy equations for Grashof numbers approaching infinity. In the case of an inclined isothermal plate the solution of the boundary-layer equations, which otherwise is adequate, but only for small inclination angles, does not explain the differences between the behaviour of the flow on both sides of the plate, which have been observed experimentally by the present author. The temperature field, but only above an inclined isothermal plate, was investigated experimentally by Rice [2], for large Grashof numbers and sufficiently good agreement with classical solution was found. For the velocity field, as far as the present author is aware, no experimental data are given in the literature. This paper presents a perturbation solution for the inclined isothermal plate free-convection problem. The solution obtained has been compared with the experimental data.

ANALYSIS

In the present case the problem is based on the finite length two-dimensional isothermal plate with both leading and trailing edges, inclined at an angle φ to the direction of the gravitational acceleration.

In the present analysis the inclination angle φ has a positive sign for the region "above" the plate and a negative sign "below" the plate.

The coordinate system, velocity directions and orientation of the plate are shown in Fig. 1.

With the assumptions that the pressure gradient in the $\bar{x}$ direction far from the plate is negligible and the physical properties of the fluid, except density, are constants, the governing Navier–Stokes, continuity and energy equations are as follows

$$\bar{u}\frac{\partial \bar{u}}{\partial \bar{x}} + \bar{v}\frac{\partial \bar{u}}{\partial \bar{y}} = -\frac{1}{\rho}\frac{\partial}{\partial \bar{x}}(\bar{p} - \bar{p}_\infty) + \nu\left(\frac{\partial^2 \bar{u}}{\partial \bar{x}^2} + \frac{\partial^2 \bar{u}}{\partial \bar{y}^2}\right) + g\beta(\bar{T} - \bar{T}_\infty)\cos\varphi \tag{1}$$

$$\bar{u}\frac{\partial v}{\partial \bar{x}} + \bar{v}\frac{\partial \bar{v}}{\partial \bar{y}} = -\frac{1}{\rho}\frac{\partial}{\partial \bar{y}}(\bar{p} - \bar{p}_\infty) + \nu\left(\frac{\partial^2 \bar{v}}{\partial \bar{x}^2} + \frac{\partial^2 \bar{v}}{\partial \bar{y}^2}\right) + g\beta(\bar{T} - \bar{T}_\infty)\sin\varphi \tag{2}$$

$$\frac{\partial \bar{u}}{\partial \bar{x}} + \frac{\partial \bar{v}}{\partial \bar{y}} = 0 \tag{3}$$

$$\bar{u}\frac{\partial}{\partial \bar{x}}(\bar{T} - \bar{T}_\infty) + \bar{v}\frac{\partial}{\partial \bar{y}}(\bar{T} - \bar{T}_\infty) = a\left[\frac{\partial^2}{\partial \bar{x}^2}(\bar{T} - \bar{T}_\infty) + \frac{\partial^2}{\partial \bar{y}^2}(\bar{T} - \bar{T}_\infty)\right]. \tag{4}$$

The boundary conditions associated with the above set of the equations are

$$\bar{y} = 0 \quad \bar{u} = 0 \quad \bar{v} = 0 \quad \bar{T} = \bar{T}_w \quad \bar{y} \to \infty \quad \bar{u} \to 0 \quad \bar{v} \to 0 \quad \bar{p} \to \bar{p}_\infty \quad \bar{T} \to \bar{T}_\infty. \tag{5}$$

After introducing the new dimensionless variables in the form

$$\bar{x} = x^+ L \qquad \bar{u} = u^+ \frac{\nu}{L} N_{Gr}$$

$$\bar{y} = y^+ L \qquad \bar{v} = v^+ \frac{\nu}{L} N_{Gr}$$

$$\bar{T} - \bar{T}_\infty = \bar{T}^+ (\bar{T}_w - \bar{T}_\infty)$$

$$\bar{p} - \bar{p}_\infty = p^+ \frac{\rho \nu^2}{L^2} N_{Gr}$$

where the Grashof number is defined as

$$N_{Gr} = \frac{g\beta(\bar{T}_w - \bar{T}_\infty) L^3 \cos\varphi}{\nu^2}$$

and if the dimensionless stream function which satisfies identically the continuity equation (3) is taken as

$$u^+ = \frac{\partial \psi^+}{\partial y^+} \qquad v^+ = -\frac{\partial \psi^+}{\partial x^+}$$

equations (1, 2) and (4) became

$$N_{Gr}\left(\frac{\partial \psi^+}{\partial y^+}\cdot\frac{\partial^2 \psi^+}{\partial x^+ \partial y^+} - \frac{\partial \psi^+}{\partial x^+}\cdot\frac{\partial^2 \psi^+}{\partial y^{+2}}\right) = -\frac{\partial p^+}{\partial x^+} + \left(\frac{\partial^3 \psi^+}{\partial x^{+2}\partial y^+} + \frac{\partial^3 \psi^+}{\partial y^{+3}}\right) + \bar{T}^+ \tag{6}$$

$$N_{Gr}\left(-\frac{\partial \psi^+}{\partial y^+}\cdot\frac{\partial^2 \psi^+}{\partial x^{+2}} + \frac{\partial \psi^+}{\partial x^+}\cdot\frac{\partial^2 \psi^+}{\partial x^+ \partial y^+}\right) = -\frac{\partial p^+}{\partial y^+} + \left(\frac{\partial^3 \psi^+}{\partial x^{+3}} + \frac{\partial^3 \psi^+}{\partial x^+ \partial y^{+2}}\right) + \bar{T}^+ \tan\varphi \tag{7}$$

$$N_{Gr}\left(\frac{\partial\psi^+}{\partial y^+}\cdot\frac{\partial\overline{T}^+}{\partial x^+}-\frac{\partial\psi^+}{\partial x^+}\cdot\frac{\partial\overline{T}^+}{\partial y^+}\right)=N_{Pr}^{-1}\left(\frac{\partial^2T^+}{\partial x^{+2}}+\frac{\partial^2T^+}{\partial y^{+2}}\right).\tag{8}$$

From the boundary-layer theory it is known that the ratios $\bar{y}/\bar{x}$ and $\bar{v}/\bar{u}$ are of the same order of magnitude as $N_{Gr}^{-\frac{1}{4}}$. Therefore the new set of independent variables X and Y, and the dependent

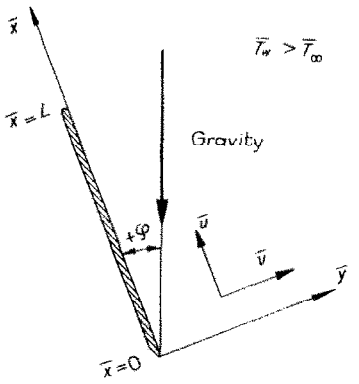

FIG. 1. The plate coordinate system.

functions $\theta(X, Y)$, $P(X, Y)$ and $\Psi(X, Y)$ can be defined in such a way that the ratios Y/X and

$$\frac{\partial\Psi}{\partial X}\Big/\frac{\partial\Psi}{\partial Y}$$

are of the order of unity.

Hence we have:

$$\begin{aligned}X&=x^+\\Y&=y^+N_{Gr}^{-\frac{1}{4}}\\\Psi(X,Y)&=\psi^+N_{Gr}^{\frac{3}{4}}\\P(X,Y)&=p^+\\\theta(X,Y)&=T^+.\end{aligned}\tag{9}$$

Introduction of (9) into the equations (6–8) transforms them to

$$\frac{\partial\Psi}{\partial Y}\cdot\frac{\partial^2\Psi}{\partial X\partial Y}-\frac{\partial\Psi}{\partial X}\cdot\frac{\partial^2\overline{\Psi}}{\partial Y^2}=-\frac{\partial P}{\partial X}+N_{Gr}^{-\frac{1}{4}}\frac{\partial^3\Psi}{\partial X^2\partial Y}+\frac{\partial^3\Psi}{\partial Y^3}+\theta\tag{10}$$

$$N_{Gr}^{-\frac{1}{4}}\left(-\frac{\partial\Psi}{\partial Y}\cdot\frac{\partial^2\Psi}{\partial X^2}+\frac{\partial\Psi}{\partial X}\cdot\frac{\partial^2\Psi}{\partial X\partial Y}\right)=-\frac{\partial P}{\partial Y}-N_{Gr}^{-1}\frac{\partial^3\Psi}{\partial X^3}+-N_{Gr}^{-\frac{1}{2}}\frac{\partial^3\Psi}{\partial X\partial Y^2}+N_{Gr}^{-\frac{1}{4}}\theta\tan\varphi\tag{11}$$

$$\frac{\partial\Psi}{\partial Y}\cdot\frac{\partial\theta}{\partial X}-\frac{\partial\Psi}{\partial Y}\cdot\frac{\partial\theta}{\partial Y}=N_{Pr}^{-1}\left(N_{Gr}^{-\frac{1}{2}}\frac{\partial^2\theta}{\partial X^2}+\frac{\partial^2\theta}{\partial Y^2}\right)\tag{12}$$

which are similar to those discussed by Yang [1]. The perturbation solution is now constructed by letting

$$\Psi=\Psi^{(0)}+N_{Gr}^{-\frac{1}{4}}\Psi^{(1)}+\ldots\tag{13}$$

$$\theta=\theta^{(0)}+N_{Gr}^{-\frac{1}{4}}\theta^{(1)}+\ldots\tag{14}$$

$$P=P^{(0)}+N_{Gr}^{-\frac{1}{4}}P^{(1)}+\ldots\tag{15}$$

where $N_{Gr}^{-\frac{1}{4}}$ is taken as a small constant parameter, based on boundary-layer solution. When the above expansions are substituted in equations (10–12) and the coefficients of like powers of N_{Gr} are collected, the following sets of equations for the zeroth-order and first-order approximations may be formed.

The zeroth-order approximation:

$$\frac{\partial \Psi^{(0)}}{\partial Y} \cdot \frac{\partial^2 \Psi^{(0)}}{\partial X \partial Y} - \frac{\partial \Psi^{(0)}}{\partial X} \cdot \frac{\partial^2 \Psi^{(0)}}{\partial Y^2} = -\frac{\partial P^{(0)}}{\partial X} + \frac{\partial^3 \Psi^{(0)}}{\partial Y^3} + \theta^{(0)} \tag{16}$$

$$-\frac{\partial P^{(0)}}{\partial Y} = 0 \tag{17}$$

$$\frac{\partial \Psi^{(0)}}{\partial Y} \cdot \frac{\partial \theta^{(0)}}{\partial X} - \frac{\partial \Psi^{(0)}}{\partial X} \cdot \frac{\partial \theta^{(0)}}{\partial Y} = N_{Pr}^{-1} \frac{\partial^2 \theta^{(0)}}{\partial Y^2} \tag{18}$$

The first-order approximation:

$$\frac{\partial \Psi^{(0)}}{\partial Y} \cdot \frac{\partial^2 \Psi^{(1)}}{\partial X \partial Y} + \frac{\partial^2 \Psi^{(0)}}{\partial X \partial Y} \cdot \frac{\partial \psi^{(1)}}{\partial Y} - \left(\frac{\partial \Psi^{(0)}}{\partial X} \cdot \frac{\partial^2 \Psi^{(1)}}{\partial Y^2} + \frac{\partial^2 \Psi^{(0)}}{\partial Y^2} \cdot \frac{\partial \Psi^{(1)}}{\partial X} \right) = -\frac{\partial P^{(1)}}{\partial X} + \frac{\partial^3 \Psi^{(1)}}{\partial Y^3} + \theta^{(1)} \tag{19}$$

$$-\frac{\partial P^{(1)}}{\partial Y} + \theta^{(0)} \tan \varphi = 0 \tag{20}$$

$$\frac{\partial \Psi^{(0)}}{\partial Y} \cdot \frac{\partial \theta^{(1)}}{\partial X} + \frac{\partial \theta^{(0)}}{\partial X} \cdot \frac{\partial \Psi^{(0)}}{\partial Y} - \left(\frac{\partial \Psi^{(0)}}{\partial X} \cdot \frac{\partial \theta^{(1)}}{\partial Y} + \frac{\partial \theta^{(0)}}{\partial Y} \cdot \frac{\partial \Psi^{(1)}}{\partial X} \right) = N_{Pr}^{-1} \frac{\partial^2 \theta^{(1)}}{\partial Y^2}. \tag{21}$$

After letting $P^{(0)}(X, Y) \equiv 0$ and by introducing

$$\eta = Y(4X)^{-\frac{1}{4}} \qquad \Psi^{(0)} = (4X)^{\frac{1}{4}} F(\eta) \qquad \theta^{(0)} = H(\eta) \tag{22}$$

the set of equations (16–18) reduces to the well known set of ordinary nonlinear equations

$$\begin{aligned} F''' + 3FF'' - 2F'^2 + H &= 0 \\ H'' + 3N_{Pr} FH' &= 0 \end{aligned} \tag{23}$$

satisfying the boundary conditions

$$\eta = 0 \qquad F' = 0 \qquad F = 0 \qquad H = 1 \qquad \eta \to \infty \qquad F' \to 0 \qquad H \to 0$$

where primes indicate derivatives with respect to η. To get the solution of the first-order perturbation equations (19–21) the standard technique used in boundary-layer analysis may be conveniently employed. To obtain non-homogeneous boundary conditions for the above set of equations (they are homogeneous and with homogeneous physical boundary conditions give only trivial solutions) the solution for the potential flow region outside the boundary layer must be found. By considering the outer edge of the boundary layer as a plane sink, with the sink strength proportional to the normal velocity component v_∞, the complex velocity potential may be obtained as follows

$$U^{(1)} - iV^{(1)} = \frac{3F(\infty)}{\pi(4)^{\frac{1}{4}}} \left[\frac{\pi i}{Z^{\frac{1}{4}}} + \frac{1}{Z^{\frac{1}{4}}} \ln \left(\frac{1 - Z^{\frac{1}{4}}}{1 + Z^{\frac{1}{4}}} \right) + \frac{2}{Z^{\frac{1}{4}}} \arctan \left(\frac{1}{Z^{\frac{1}{4}}} \right) \right]. \tag{24}$$

For $Z = X$, because we are only interested in the values of $U^{(1)}$ for $\bar{y} = 0$, the potential flow

velocity component in the $\bar{x}$ direction (written in series form convergent for $0 < X < 1$) may be obtained

$$U^{(1)} = \frac{3F(\infty)}{\pi(4X)^{\frac{1}{4}}}\left[\pi - \sum_{m=0}^{\infty} \frac{X^{m+\frac{1}{4}}}{m+\frac{1}{4}}\right]. \tag{25}$$

Assuming the boundary layer as very thin, we see from the definition that $U^{(1)}$ must be the limit of $\partial\Psi^{(1)}/\partial Y$ for $Y \to \infty$, hence

$$\Psi^{(1)} = \frac{3F(\infty)}{\pi}\left[\pi f(\eta) - \sum_{m=0}^{\infty} \frac{X^{m+\frac{1}{4}}}{m+\frac{1}{4}} f_m(\eta)\right] \tag{26}$$

and similarly

$$\theta^{(1)} = \frac{3F(\infty)}{\pi}(4X)^{-\frac{1}{4}}\left[\pi h(\eta) - \sum_{m=0}^{\infty} \frac{X^{m+\frac{1}{4}}}{m+\frac{1}{4}} h_m(\eta)\right] \tag{27}$$

$$P^{(1)} = \frac{3F(\infty)}{\pi}(4X)^{\frac{1}{4}}\left[\pi p(\eta) - \sum_{m=0}^{\infty} \frac{X^{m+\frac{1}{4}}}{m+\frac{1}{4}} p_m(\eta)\right]. \tag{28}$$

If the foregoing equations are substituted in the equations (19–21) and the coefficients of like powers of X are collected the following set of ordinary differential equations may be obtained:

$$\left.\begin{aligned} &f''' + 3Ff'' - F'f' - p + \eta p' + h = 0\\ &-3F(\infty)p' + H\tan\varphi = 0\\ &h'' + 3N_{Pr}(Fh)' = 0 \end{aligned}\right\} \tag{29}$$

$$\left.\begin{aligned} &f_m''' + 3Ff_m'' - 2(2m+1)F'f_m' + (4m+1)F''f_m - 2(2m+1)p_m + \eta p_m' + h_m = 0\\ &p_m' = 0\\ &h_m'' + N_{Pr}[3Fh_m' - 2(2m-1)F'h_m + (4m+1)H'f_m] = 0\\ &\qquad m = 0, 1, 2, 3, \ldots \end{aligned}\right\} \tag{30}$$

with the following boundary conditions

$$\left.\begin{aligned} &\eta = 0, f = f' = 0, h = 0\\ &\eta \to \infty, f' \to 1, h \to 0, p \to 0 \end{aligned}\right\} \tag{31}$$

$$\left.\begin{aligned} &\eta = 0, f_m = f_m' = 0, h_m = 0\\ &\eta \to \infty, f_m' \to 1, h_m \to 0, p_m \to 0. \end{aligned}\right\} \tag{32}$$

It may be easily shown that for the boundary conditions (31) and (32) $h(\eta) \equiv 0$ and $p_m(\eta) \equiv 0$ for all values of m. Equations (30) are similar to those obtained by Yang [1] for the vertical plate problem. The above equations do not appear to have closed-form solutions, and consequently can only be solved numerically.

Numerical solutions to the sets of equations (23, 29) and (30), have been carried out on Elliott 803 digital computer for Prandtl number $N_{Pr} = 0{\cdot}7$ and nine inclination angles $\varphi = 0, \pm 15°,$

$\pm 30°$, $\pm 45°$, $\pm 60°$. The results of calculations are shown on Figs. 2 and 3, which contain functions $f'(\eta)$ and $p(\eta)$ only, because functions $f_m(\eta)$ and $h_m(\eta)$ are identical with those described in [1]. From the second equation in the set (29) it is evident that

$$-p(\eta, -\varphi) = p(\eta, \varphi).$$

Numerical values of surface derivatives for $N_{Pr} = 0{\cdot}7$ and various inclination angles are given in Table 1.

The local velocity profiles for both components of flow field may be determined from definitions and equation (13) after neglecting the second and higher order terms of parameter $N_{Gr}^{-\frac{1}{4}}$ as

$$\bar{u}\frac{L}{\nu}(4XN_{Gr})^{-\frac{1}{4}} = F'(\eta) + N_{Gr}^{-\frac{1}{4}}\frac{3F(\infty)}{\pi(4X)^{\frac{1}{4}}}\left[\pi f'(\eta) - \sum_{m=0}^{\infty}\frac{X^{m+\frac{1}{4}}}{m+\frac{1}{4}}f'_m(\eta)\right] \tag{33}$$

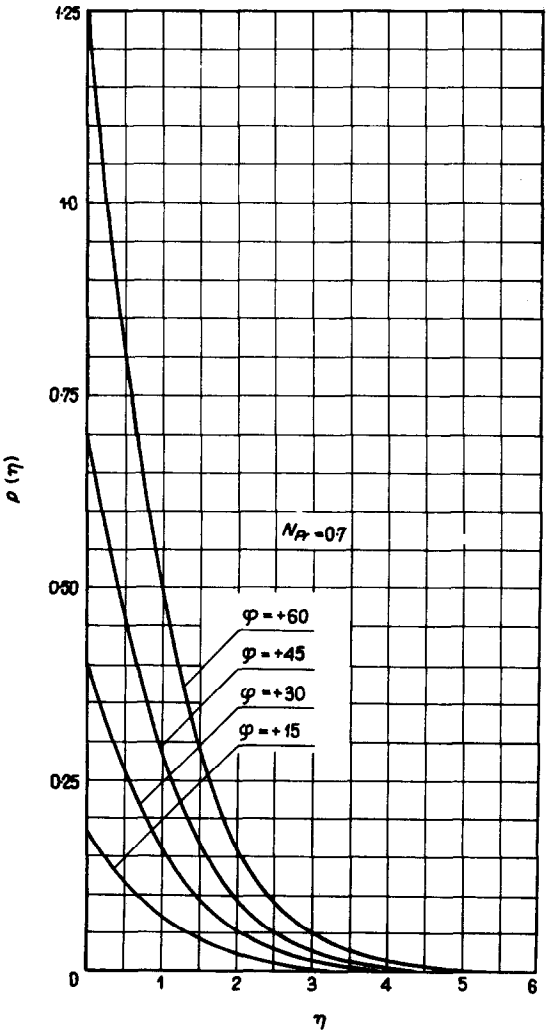

FIG. 2. Dimensionless pressure function $p(\eta)$ for $N_{Pr} = 0{\cdot}7$ and various inclination angles.

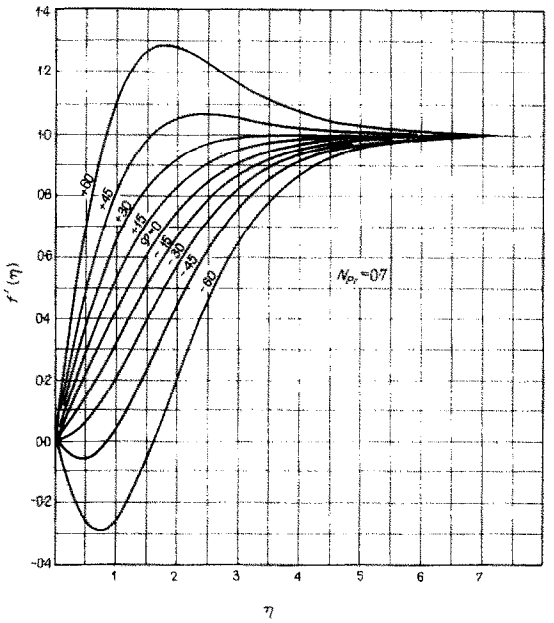

FIG. 3. Dimensionless function $f'(\eta)$ for $N_{Pr} = 0{\cdot}7$ and various inclination angles.

$$\bar{v}\frac{L}{\nu}\left(\frac{N_{Gr}}{4X}\right)^{-\frac{1}{4}} = \eta F'(\eta) - 3F(\eta) + N_{Gr}^{-\frac{1}{4}}\frac{3F(\infty)}{\pi(4X)^{\frac{1}{4}}}\left\{\pi\eta f'(\eta) + \right.$$

$$\left. - \sum_{m=0}^{\infty}\frac{X^{m+\frac{1}{4}}}{m+\frac{1}{4}}\left[\eta f'_m(\eta) - (4m+1)f_m(\eta)\right]\right\}. \tag{34}$$

The local temperature profiles may be determined similarly, and are given by

$$\frac{\bar{T} - \bar{T}_\infty}{\bar{T}_w - \bar{T}_\infty} = H(\eta) + N_{Gr}^{-\frac{1}{4}}\frac{3F(\infty)}{\pi(4X)^{\frac{1}{4}}}\left[-\sum_{m=0}^{\infty}\frac{X^{m+\frac{1}{4}}}{m+\frac{1}{4}}h_m(\eta)\right]. \tag{35}$$

Local rates of heat transfer may now be determined from equation (35) by differentation, and if a local coefficient of heat transfer will be defined as

$$\alpha(\bar{T}_w - \bar{T}_\infty) = -\lambda_w\left(\frac{\partial T}{\partial \bar{y}}\right)_w$$

it may be shown that

$$\bar{N}_{Nu} = [-H'(0)]\left(\frac{\bar{N}_{Gr}}{4}\right)^{\frac{1}{4}}(\cos\varphi)^{\frac{1}{4}} + \frac{3F(\infty)}{4\pi}\sum_{m=0}^{\infty}\frac{X^{m+\frac{1}{4}}}{m+\frac{1}{4}}h'_m(0). \tag{36}$$

A comparison of the equations (33–36) with the author's experimental data for some chosen values of variable X and various inclination angles φ will be made in the next section.

Table 1. Surface derivatives

φ	$p(0)$	$f''(0)$
0	0·0	0·443109
+15	0·187503	0·639893
−15	−0·187503	0·246325
+30	0·404013	0·867090
−30	−0·404013	0·019110
+45	0·699771	1·177479
−45	−0·699771	−0·291260
+60	1·212039	1·715200
−60	−1·212039	−0·828980

m	$f''_m(0)$	$h'_m(0)$
0	0·157485	−0·132668
1	0·014812	−0·088903
2	0·001963	−0·045271
3	0·000321	−0·024513
4	0·000130	−0·014011
5	−0·000107	−0·008193

$N_{Pr} = 0{\cdot}7$, $F''(0) = 0{\cdot}678891$, $H'(0) = -0{\cdot}499482$, $F\infty) = 0{\cdot}604597$.

COMPARISON WITH EXPERIMENTAL DATA

Experimental data for the local velocity profiles in laminar free convection along an inclined plate are not known in the literature as far as the present author is aware, although temperature measurements, local and overall heat-transfer characteristics have been reported [4].

In order to test the validity of the present theory, local velocity and temperature profiles were measured by means of a Mach–Zender interferometer and by means of the technique reported in [8]. The measurements were done in air, on the copper plate 25-cm high and 25-cm wide. It was observed that the flow in the boundary layer was completely laminar, except for the region near the trailing edge—above $X = \frac{3}{4}$ (for large inclination angles $+30°$ and $+45°$) "above" the plate. Since the present theory is only valid for laminar flow and the experimental data in the upper part of the plate have been influenced by the observed instability waves, comparison will be made between the analytical results and experimental data for the lower portion of the plate. To evaluate the physical properties of the air, the reference temperature formula recommended by Sparrow and Gregg [7] was used as follows:

$$\bar{T}_r = \bar{T}_w - 0{\cdot}38\,(\bar{T}_w - \bar{T}_\infty);\beta = \frac{1}{\bar{T}_\infty}. \tag{37}$$

With $\bar{T}_r = 36{\cdot}5°C$ (constant for all experiments with an accuracy of $\pm 0{\cdot}1$ degC), the corresponding Grashof number and expansion coefficient [equations (13–15)] were as follows: $(4{\cdot}265 \pm 0{\cdot}03) \cdot 10^7$ $(\cos\varphi)$ and $0{\cdot}01235$ $(\cos\varphi)^{-\frac{1}{4}}$. Numerical calculations of equations (33–35) have been carried out for $X = \frac{1}{24}, \frac{1}{5}, \frac{1}{2}$ and $\frac{3}{4}$ (except for $X = \frac{5}{6}, \frac{7}{8}$ and the inclination angle ± 45) and for the inclination angles $\varphi = 0, \pm 15, \pm 30, \pm 45°$, for which the local velocity and temperature profiles were measured. Comparisons between the present theory and the measured data for some chosen values of X and inclination angles φ are shown in Figs. 4–7 for the velocity field and in Fig. 8 for

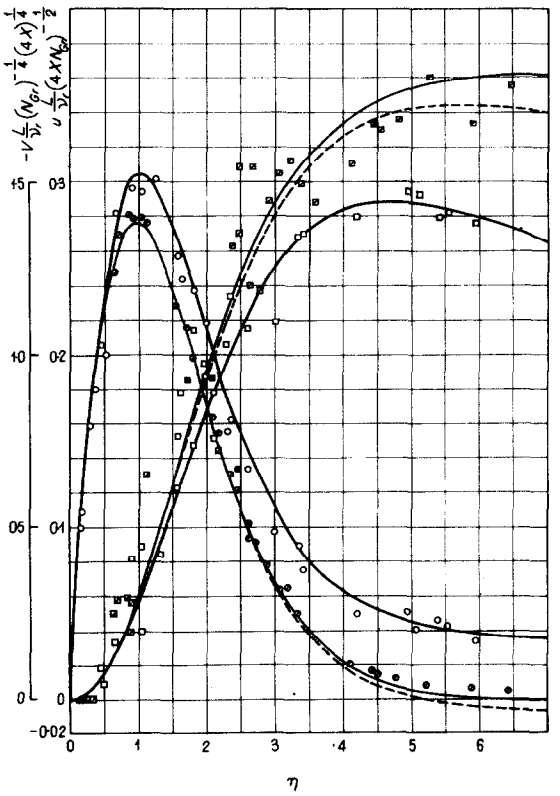

FIG. 4. Comparison of dimensionless local velocity profiles for $\varphi = 0°$ and $X = \frac{1}{24}$, $X = \frac{3}{4}$ with experimental data (present solution ——— ○□ $X = \frac{1}{24}$; — — — ⊘⊡ $X = \frac{3}{4}$; ——— boundary-layer solution).

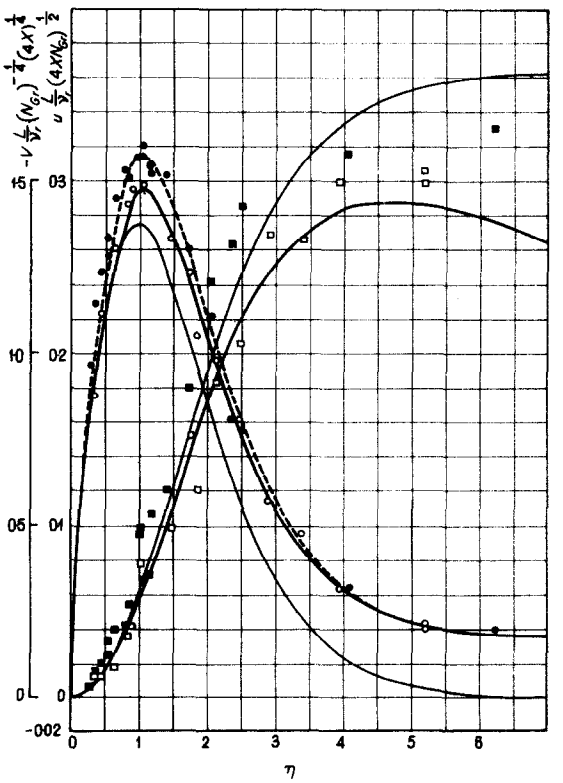

FIG. 5. Comparison of dimensionless local velocity profiles for $\varphi = 15°$ and $X = \frac{1}{24}$ with experimental data (present solution ——— ○□ $\varphi = -15°$; — — — ●■ $\varphi = +15°$; ——— boundary-layer solution).

the temperature field. For the temperature profiles, Fig. 8 shows only the calculated curve for $X = \frac{1}{24}$, because the corresponding curves for other values of X all lie between the curve for $X = \frac{1}{24}$ and the profile from boundary-layer solution. Figure 9 shows a plot of local Nusselt number $\bar{N}_{Nu}$ against local Grashof number $\bar{N}_{Gr}$ for the inclination angles $\varphi = 0$ and $\varphi = \pm 45$ ("above" and "under" the plate). Figure 10 shows a photograph typical of the technique of measuring the flow field characteristics [8].

CONCLUDING REMARKS

This paper presents a perturbation analysis for the problem of laminar free convection along an inclined plate, utilizing the classical boundary-layer solution as the zeroth-order approximation. The first order perturbation for the velocity and temperature fields have been calculated in detail for the Prandtl number $N_{Pr} = 0{\cdot}7$ and inclination angles $\varphi = 0, \pm 15, \pm 30, \pm 45$ and ± 60. Comparison of the calculated results with the experimental data confirmed the validity of the analysis. The differences in flow behaviour on both sides of the plate have been explained by the opposite signs of the pressure function $p(\eta)$ (Fig. 2), which strongly affects function $f'(\eta)$ (Fig. 3) which in turn has a predominant influence on the flow field characteristics. The slight deviations between

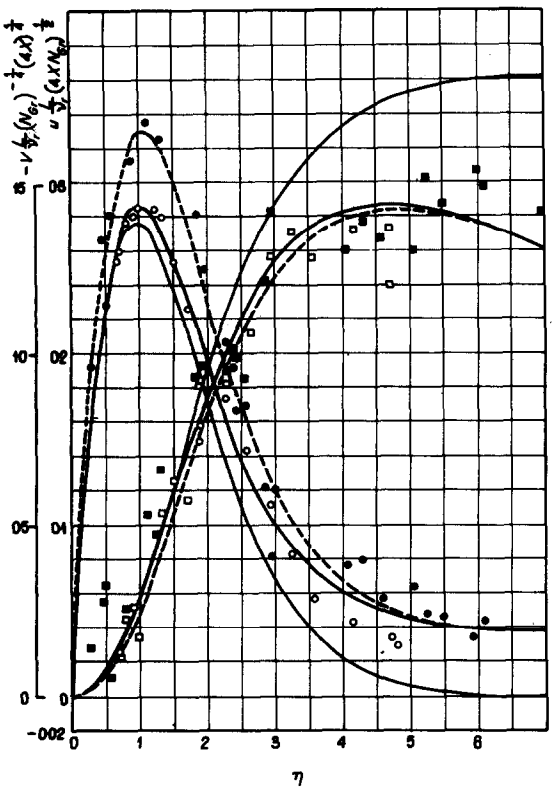

FIG. 6. Comparison of dimensionless local velocity profiles for $\varphi = 30°$ and $X = \frac{1}{24}$ with experimental data (present solution ——— ○□ $\varphi = -30°$; — — — ●■ $\varphi = +30°$; ——— boundary-layer solution).

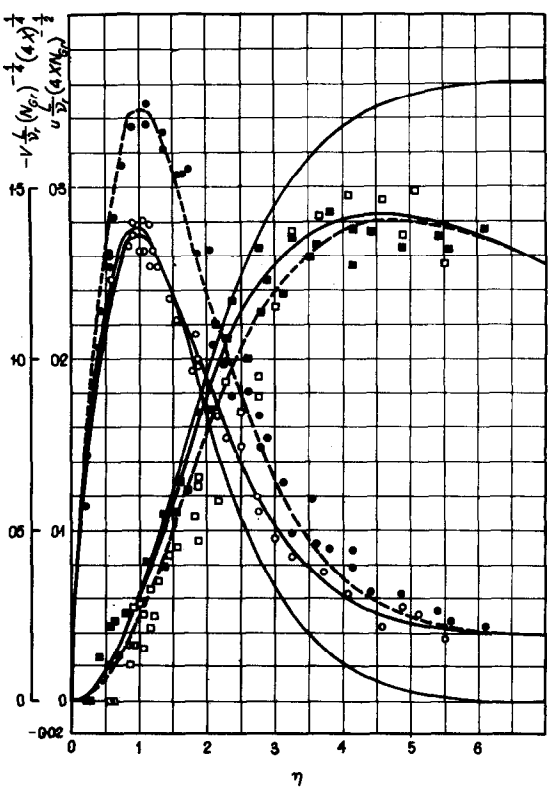

FIG. 7. Comparison of dimensionless local velocity profiles for $\varphi = 45°$ and $X = \frac{1}{24}$ with experimental data (present solution ——— ○□ $\varphi = -45°$; — — — ●■ $\varphi = +45°$; ——— boundary-layer solution).

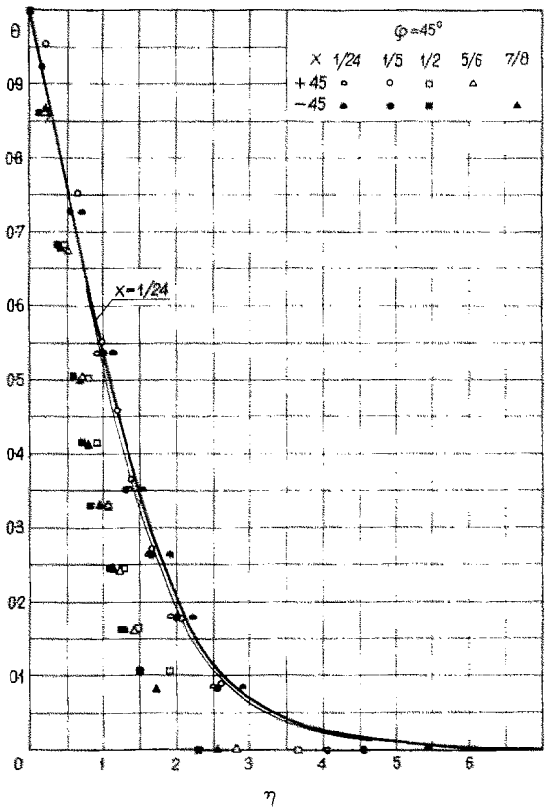

FIG. 8. Comparison of dimensionless temperature profiles for $\varphi = 45°$ and various values of X coordinate (present solution ——— $X = \frac{1}{24}$; ——— boundary-layer solution).

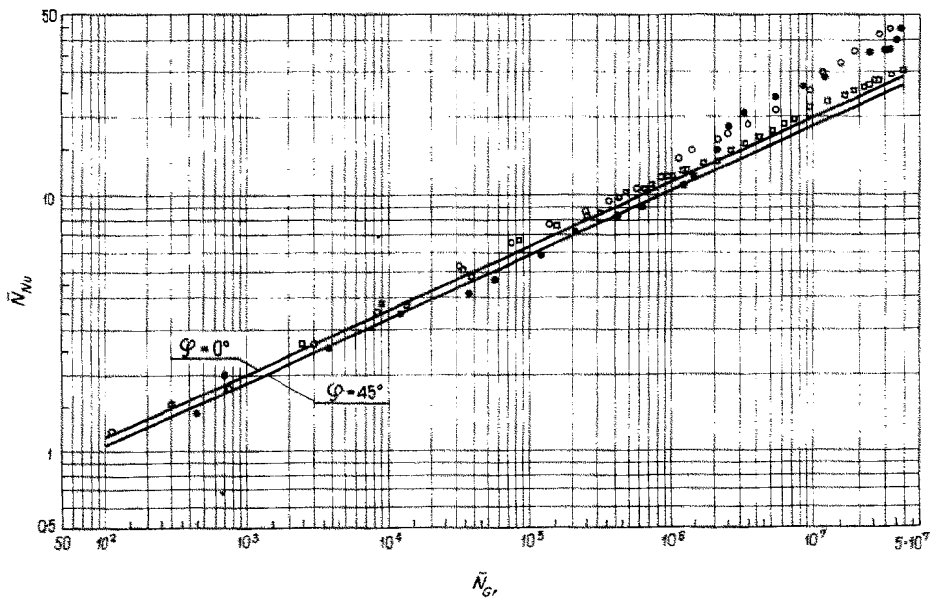

FIG. 9. Comparison of local Nusselt numbers $\bar{N}_{Nu}$ for $\varphi = 0°$ and $\varphi = 45°$ (□ $\varphi = 0°$; ● $\varphi = +45°$; ○ $\varphi = -45°$).

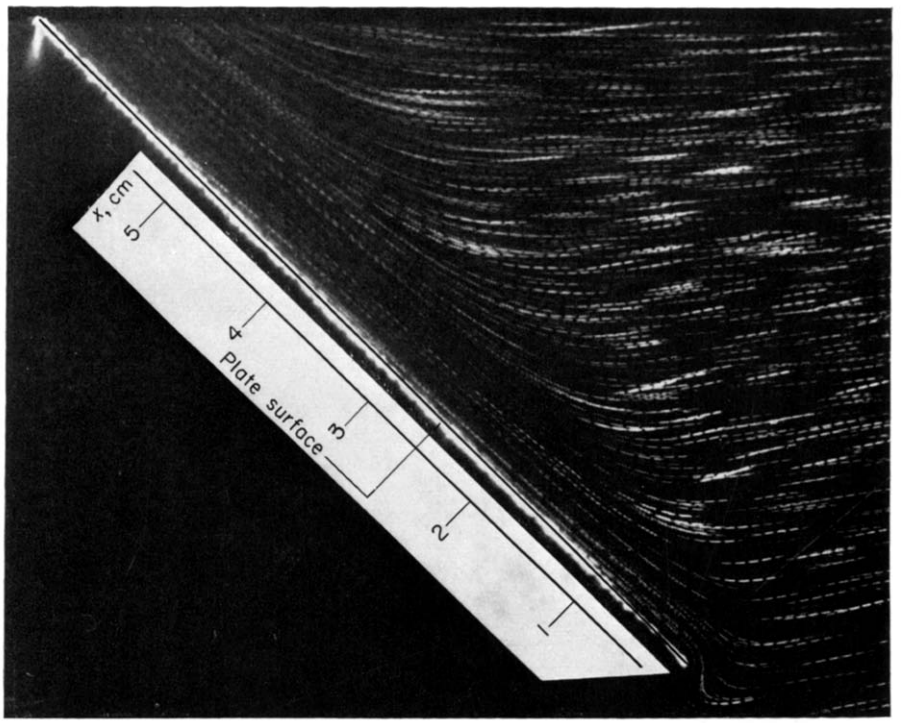

FIG. 10. Typical photograph for the technique of measurements flow field characteristics [8] ($\varphi = +45°$, leading edge of the plate, $\bar{T}_w = 45{\cdot}7°C$, $\bar{T}_\infty = 20{\cdot}9°C$, exposition time approximately 0·5 s).

the measured data and the present analytical theory could be attributed to the degree of experimental error in the experiments. As one can see from the temperature field obtained, the present analysis hardly brings any change to the temperature profile obtained from the solution of the boundary layer. This fully explains the good agreement between the boundary-layer solution and the experimental data for values of $X < \frac{1}{2}$, that is, in the region where stability has not yet been observed.

REFERENCES

1. K. T. YANG and E. W. JERGER, First-order perturbations of laminar free-convection boundary layers on a vertical plate, *J. Heat Transfer* **86**, 107–115 (1964).
2. Y. H. KUO, On the flow of an incompressible viscous fluid past a flat plate at moderate Reynolds numbers, *J. Math. Phys.* **32**, 83–101 (1954).
3. M. J. LIGHTHILL, A technique for rendering approximate solutions to physical problems uniformly valid, *Phil. Mag.* **40**, 1179–1201 (1949).
4. B. R. RICH, An investigation of heat transfer from an inclined flat plate in free convection, *Trans. Am. Soc. Mech. Engrs* **75**, 489–497 (1953).
5. G. S. H. LOCK, Steady laminar free convection from inclined arbitrary shaped plane surface, *Int. J. Heat Mass Transfer* **7**, 669–671 (1964).
6. S. Ostrach, An analysis of laminar free-convection flow and heat transfer about a flat plate parallel to the direction of the generating body force, NACA TR 1111 (1953).
7. E. M. SPARROW and J. L. GREGG, The variable fluid-property problem in free convection, *Trans. Am. Soc. Mech. Engrs* **80**, 879–886 (1958).
8. K. BRODOWICZ and W. T. KIERKUS, Determination of streamlines and velocity components in free convection, *Arch. Budowy Masz.* **12**, 473–486 (1965).
9. W. W. MALOZIEMOW and J. A. TURCZYN, Investigation of the temperature fields by means of the interferometer, *Inzh. Fiz. Zh.* **8**, 182–185 (1965).

Résumé—On présente ici une analyse théorique par la méthode des perturbations pour la convection naturelle laminaire bidimensionnelle le long d'une plaque isotherme inclinée, en employant la solution du type de la couche limite classique comme approximation d'ordre zéro. La solution de perturbation du premier ordre a été trouvée pour les champs de vitesse et de température. Les distributions à la fois des composantes du champ de vitesse et du champ de température calculées en détail pour un nombre de Prandtl de 0,7 et des inclinaisons de 0°, ±15°, ±30°, et ±45° sont comparées avec les données expérimentales. On a trouvé un bon accord entre la solution théorique et les résultats expérimentaux.

Zusammenfassung—Die Arbeit behandelt eine Störanalyse für zweidimensionale laminare freie Konvektion entlang einer geneigten isothermen Platte auf Grund der klassischen Grenzschichtlösung als Näherung nullter Ordnung. Eine Störlösung erster Ordnung liess sich für Geschwindigkeits- und Temperaturfelder finden. Die für die Prandtl-Zahl 0,7 und für Neigungswinkel $= 0° \pm 15° \pm 30° \pm 45°$ berechneten Verteilungen beider Komponenten des Geschwindigkeits- und Temperaturfeldes wurden mit Versuchswerten verglichen. Gute Übereinstimmung ergab sich zwischen der theoretischen Lösung und den Versuchsergebnissen.

Аннотация—В данной статье приводится анализ двумерной ламинарной свободной конвекции вблизи наклонной изотермической пластины методом «возмущения» уравнений пограничного слоя. При этом, классическое решение, построенное по теории пограничного слоя, используется в качестве нулевого приближения. В работе найдено решение для профилей скорости и температуры на основе уравнений, представляющих первое приближение по отношению к уравнениям пограничного слоя. Приводится сравнение распределений обоих компонентов скоростного поля и профиля температур, детально расчитанных при $Pr = 0{,}7$ и углах наклона $\varphi = 0$, ±15, ±30, ±45, с экспериментальными данными. Найдено хорошее совпадение теоретических и экспериментальных данных.